Tunnelling and Underground Space Technology 59 (2016) 24–37

Contents lists available at ScienceDirect

Tunnelling and Underground Space Technology

journal homepage: www.elsevier.com/locate/tust

Assessment of roof stability in a room and pillar coal mine in the U.S. using three-dimensional distinct element method

T. Sherizadeh [1], Pinnaduwa H.S.W. Kulatilake *

Rock Mass Modeling and Computational Rock Mechanics Laboratories, University of Arizona, Tucson, AZ 85721, USA

ARTICLE INFO

Article history:
Received 4 October 2015
Received in revised form 16 April 2016
Accepted 8 June 2016
Available online 17 June 2016

Keywords:
Room-and-pillar mining
Roof stability
3-D discontinuum stress analysis
In-situ stress
Extraction ratio
Discontinuities

ABSTRACT

This paper examines the effect of different geological and mining factors on roof stability in underground coal mines by combining field observations, laboratory testing, and numerical modeling. An underground coal mine in western Pennsylvania is selected as a case study mine to investigate the underlying causes of roof falls in this mine. Three-dimensional distinct element analyses were performed to evaluate the effect of different parameters, such as the variation of immediate roof rock mass strength properties, variation of discontinuity mechanical properties, orientations and magnitudes of the horizontal in-situ stresses, and the size of pillars and excavations on stability of the immediate roof. The research conducted in this paper showed that the bedding planes play an important role on the geo-mechanical behavior of roofs in underground excavations. Therefore, an appropriate numerical modeling technique which incorporates the effect of discontinuities should be employed to simulate the realistic behavior of the discontinuous rock masses such as the layered materials in roof strata of the underground coal mines. The three-dimensional distinct element method used in this research showed the capability of this technique in capturing the important geo-mechanical behavior around underground excavations.

© 2016 Elsevier Ltd. All rights reserved.

1. Introduction and brief literature review

Roof falls have been one of the most common ground control problematic issues affecting the safety and economy of underground coal mines. Although, over the last decade there have been major improvements in the way which coal mines have managed the roof fall hazards through the application of safety measures, technological improvements, alternative mining methods and extensive support systems, still, roof fall accidents remain a leading cause of coal mining injuries. Roof stability is associated with the ability of the roof rock to span the openings and is dependent, in part, on the size of the opening, different rock mass material strengths and deformability, geologic discontinuity geometry and their mechanical properties, in-situ stress system, possible groundwater conditions and possible dynamic loading.

It is well known that the discontinuities not only weaken the rock masses but also they change the mechanical behavior of rock masses. The lithology of the immediate roof plays an important role on stability of the roof in underground excavations. Laminated, or thinly bedded shale, is one of the most frequently seen overlaying strata above the coal deposits. The bedding planes and interfaces have very low or close to zero tensile strength in the direction perpendicular to the bedding planes, and their shear strength is much lower than of the rock layers. As a result, the bedding planes are much weaker than the rock layers. Therefore, due to the stress concentrations caused by excavations, slippage and separation can easily happen along the bedding planes before initiation of failure within the rock layers. The slip or separation of existing discontinuities in roof strata can amplify the negative impacts of stress concentrations around underground excavations.

In the past, several attempts have been made to understand the mechanism behind the roof failure in underground coal mines. Most of these earlier attempts were based on empirical techniques and continuum based numerical methods that have limited capability in simulating the response of discontinuum rock mass behavior due to excavation. In previous studies, different factors such as the magnitude and direction of the horizontal in-situ stresses, type and mechanical properties of roof rock, surface topography, geological anomalies, gas pressure, slippage and separation of bedding planes at the roof and floor, entry width and excavation sequences are identified as key factors that could significantly impact the stability of the roof. Among all of the aforementioned factors, in spite of its importance, the impact of slip and separation of bedding planes on roof stability has not received enough attention from

* Corresponding author.
E-mail address: kulatila@u.arizona.edu (P.H.S.W. Kulatilake).
[1] Currently with Golder Associates Inc., 9 Monroe Parkway #270, Lake Oswego, OR 97035, USA.

http://dx.doi.org/10.1016/j.tust.2016.06.005
0886-7798/© 2016 Elsevier Ltd. All rights reserved.

researchers. In a few available numerical modeling studies, the bedding planes are modeled using the continuum based numerical codes such as ABAQUS (Chen, 1999) and FLAC3D (Ray, 2009). Both of the aforementioned computer programs are developed based on the continuum mechanics concepts. The continuity of deformations is the intrinsic assumption of the continuum theory and clearly it is not necessarily valid for discontinuous materials such as layered rock masses. In the presence of discontinuities, deformations can be discontinuous across the discontinuities; these displacements can be large and also the rotation of rock blocks is possible. The aforementioned two computer programs have limited capability to simulate the discontinuity behavior in a

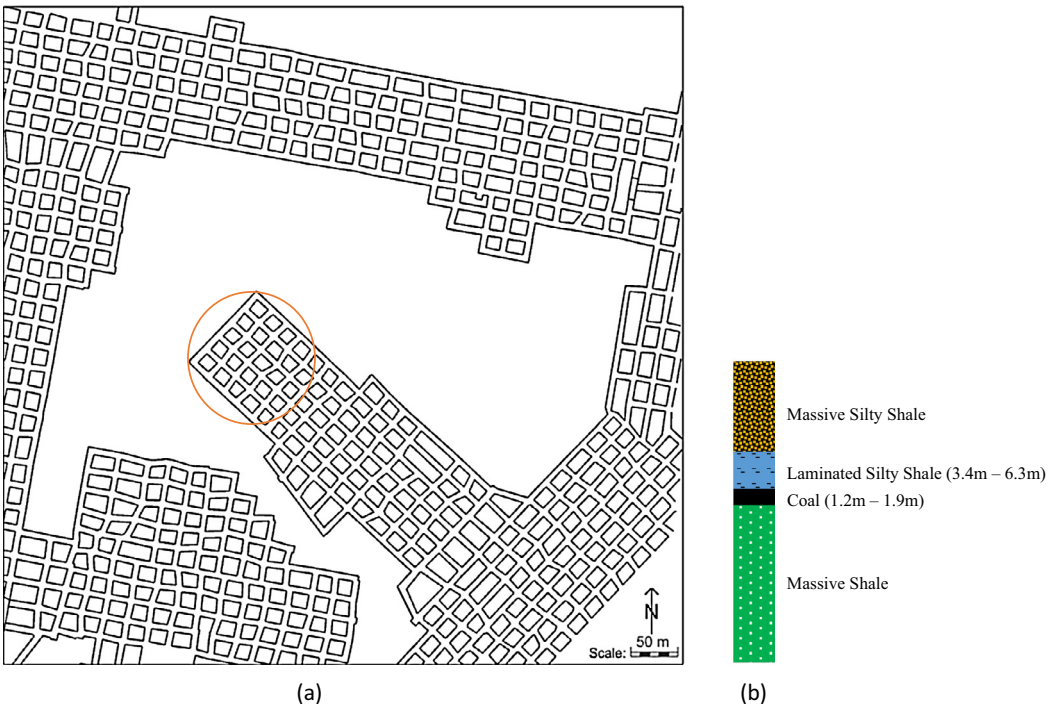

Fig. 1. (a) The plan view of the study area. (b) Typical geological column of the mine site at the study area.

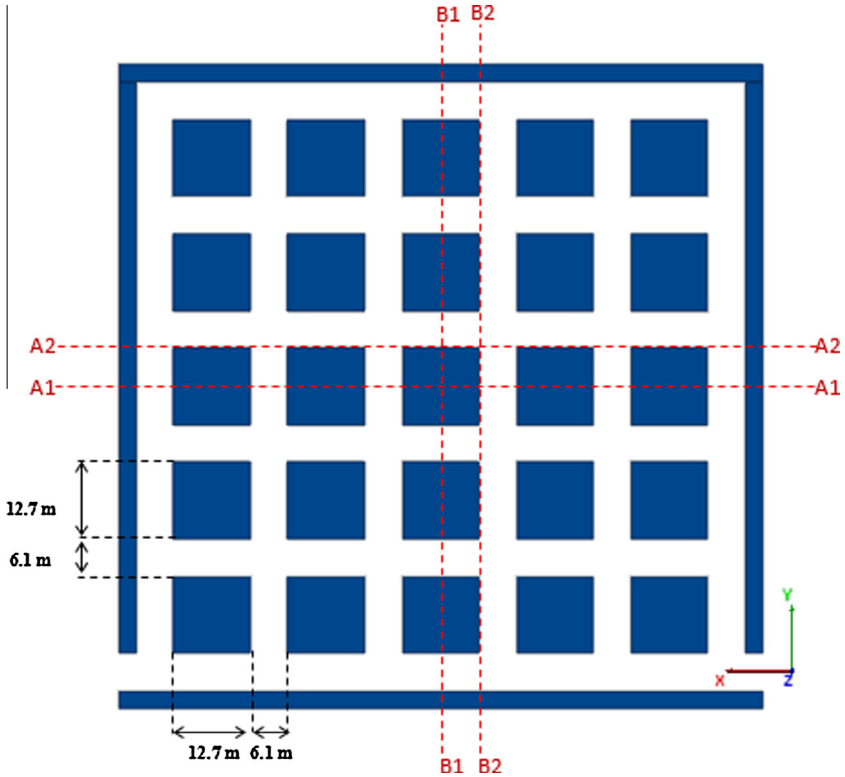

Fig. 2. The plan view of the room-and-pillar mining layout.

comprehensive manner using the interface (FLAC3D) or contact elements (ABAQUS). The validity limits, and the concerns over the computational aspects of continuum based methods for handling the discontinuous materials were the key factors convinced the authors to avoid using continuum techniques for serving the objectives of the current research.

Gadde and Peng (2005) performed three-dimensional finite difference analysis using FLAC3D software with strain softening material behavior to simulate the cutter roof in an underground coal mine. Their numerical model was fully continuum and no bedding plane was included in the model. They suggested that the strain softening material model can help to simulate the cutter roof failure up to a satisfactory level (Gadde and Peng, 2005). Chen (1999) conducted finite element analysis to study the impacts of the roof and coal interface slip and the bedding planes slip in the roof on the stress distribution in the roof strata by using the finite element analysis software named ABAQUS. To avoid the complications associated with the finite sliding between two deformable bodies, he limited his study to the two-dimensional finite element analysis (plane strain). He concluded that the slip and separation of interfaces and bedding planes have significant impact on the behavior of the roof strata and without considering the interfaces, the roof bolt functions cannot be simulated properly by using the numerical analysis methods.

The failure of underground excavations is a result of failure in both the rock mass part (consist of intact rock and minor discontinuities) and major discontinuities. In this study, the 3DEC, a three-dimensional distinct element code (Itasca, 2013), which can capture both types of aforementioned failures and their possible interactions, was used to investigate roof stability. This paper presents the results of a comprehensive study of the roof stability in a low seam mine in the U.S. to derive useful information regarding the intrinsic roof failure mechanisms. Three-dimensional distinct element analyses were performed to evaluate the effect of different parameters, such as the variation of immediate roof rock mass strength properties, variation of discontinuity mechanical properties, orientations and magnitudes of the horizontal in-situ stresses, and the size of pillars and excavations on stability of the immediate roof. Section 2 of the paper provides geological, geotechnical and mining information available on the case study. Section 3 of the paper describes the numerical modeling procedures used in the study. The obtained numerical results are covered in Section 4 of the paper. Section 5 wraps up the paper with conclusions.

2. The case study mine

In this paper, an underground coal mine in western Pennsylvania, which uses room-and-pillar mining method, was selected as a case study to investigate the underlying causes of roof falls in this mine. The case study mine had experienced more than 40 roof falls at different intensity levels over the last ten years. Based on the available data for the geometry and lithology of the interest area in the case study mine, and using the mean values of the estimated rock mass and discontinuity properties from laboratory tests, a reference model was developed. A series of parametric sensitivity analysis was then carried out to examine the impact of variation of each individual parameter on the stability of the roof. In addition to the sensitivity analyses on uncertainties associated with the rock mass and discontinuity properties, the influence of the

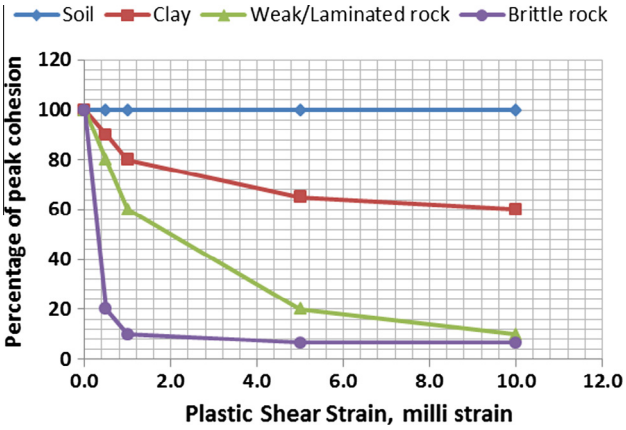

Fig. 5. Typical degradation of cohesion for different rock types with plastic strain (Ray, 2009).

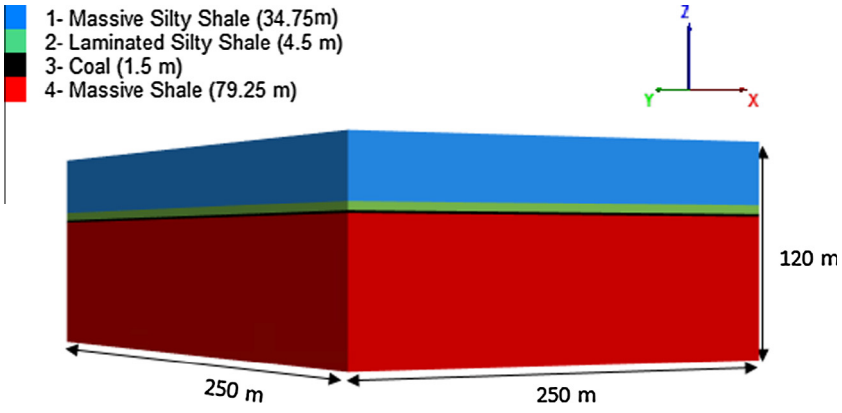

Fig. 3. Lithology used in the modeling.

Fig. 4. The location of horizontal cross-sections.

variability of the orientation and magnitude of the horizontal stresses, and the size of pillars and excavations on stability of the underground excavations have also been studied.

Table 1
The assigned rock mass property values in 3DEC.

Parameter	Values [ratios]			
	Massive silty shale	Laminated silty shale	Coal	Massive shale
Tensile strength (MPa)	2.40 [0.21]	2.40 [0.21]	1	3.30 [0.31]
Young's modulus (GPa)	8.2 [0.52]	8.2 [0.52]	3.2	13.91 [0.52]
Poisson's ratio	0.21 [1.07]	0.21 [1.07]	0.3	0.23 [1.25]
Density (kg/m^3)	2665	2665	1300	2605
Cohesion (MPa)	5.1 [0.20]	5.1 [0.20]	3.4	5.54 [0.21]
Friction angle (°)	21 [0.83]	21 [0.83]	19	22.45 [1]

Note: The values in the brackets are the ratios of the equivalent rock mass properties to the corresponding intact rock properties.

Table 2
The properties of the discontinuities used as input in the numerical modeling.

Parameter	Values for bedding	Values for interfaces	
	Laminated silty shale	Coal - laminated silty shale	Coal - massive shale
Joint friction angle (°)	17.5	18.25	18.5
Joint normal stiffness (Pa/m)	4.07E+08	3.12E+10	4.28E+10
Joint shear stiffness (Pa/m)	1.65E+07	1.94E+09	2.29E+09

2.1. Mining, geological and geotechnical parameter information for the case study mine

The case study mine uses the room-and-pillar mining method with the mining height and entry width of about 1.5 m and 6.1 m, respectively. The overburden depth ranges from 137 to 143 m. The immediate roof consists of laminated silty shale, laminated shale, or sandstone that changes from area to area, and the lithology of the immediate floor is shale or fireclay. In most of the roof failures occurred at this mine, the laminated silty shale comprises the immediate roof, and wherever the sandstone forms the immediate roof, the roof condition is good. Therefore, in this case study, the main interest was the stability of the immediate roof with laminated silty shale. The immediate roof at the case study area is mainly composed of weak laminated silty shale with thin laminations of 2.5–52 mm which fails easily along the weak laminations. These can be considered as the major discontinuities for the study area. No information is available for the minor discontinuities (small scale joints) for the studied area. The plan view of the study area is shown in Fig. 1a. A typical geological column of the mine site at the study area is also shown in Fig. 1b. It provides the possible ranges for the critical layers (coal and laminated silty shale) in regards to investigating stability around the excavated coal seam.

Extensive laboratory tests were performed on the core samples obtained from the case study mine, at the University of Arizona Rock Mechanics Laboratory. Brazilian tensile test, unconfined compressive strength (UCS) test, triaxial compression test, direct shear test of discontinuities, and a specially designed test to estimate the joint normal stiffness were conducted on the prepared samples to obtain the intact rock and discontinuity mechanical properties of different rock types of the case study mine.

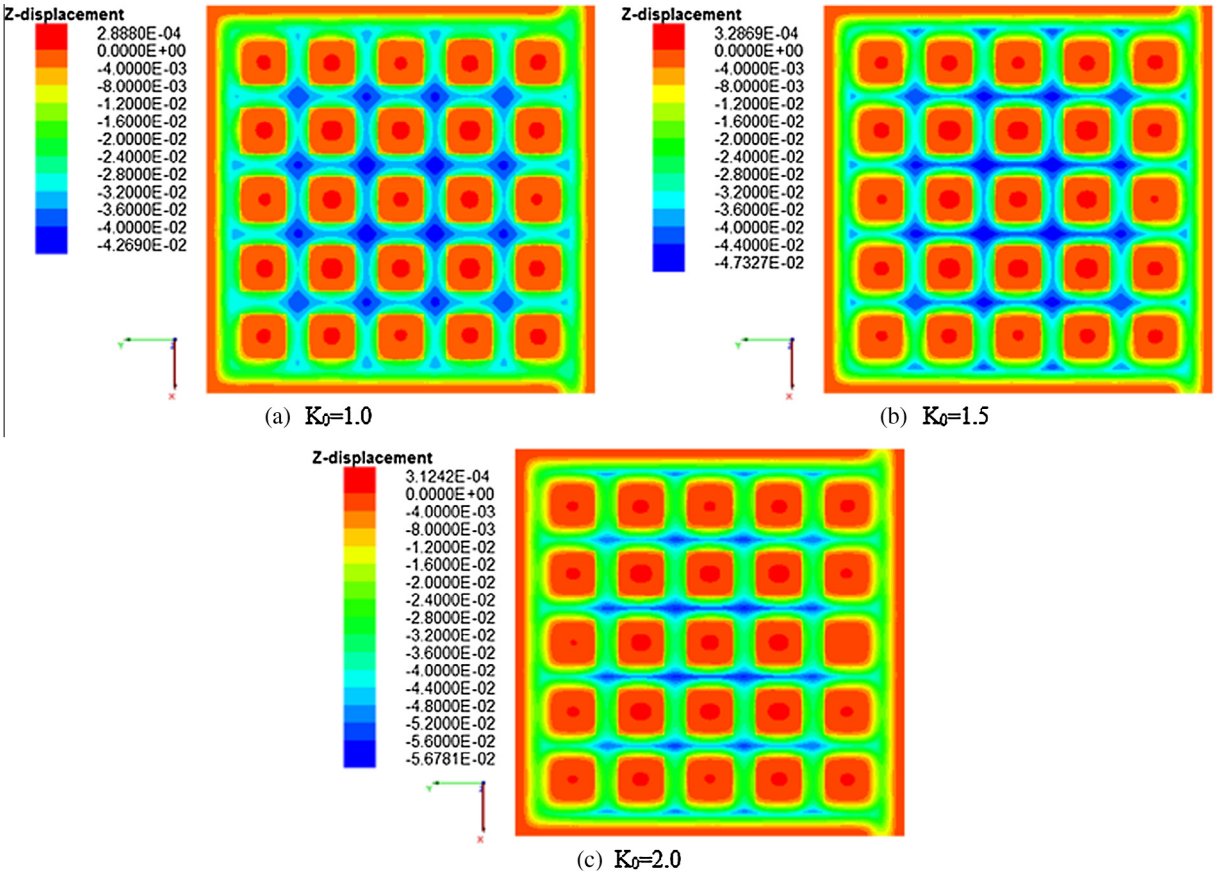

Fig. 6. The Z-displacement distribution at the roofline on cross section C-C for different values of K0.

3. Numerical modeling

3.1. Model geometry, lithology, mesh, boundary, and in-situ stress conditions

A three-dimensional reference model was built as much as possible with symmetrical geometry to allow for easy assessment of the influence of each individual variable in parametric studies. The reference model was built with 25 pillars (5 in x-direction and 5 in y-direction), six entries and six crosscuts. Both the entries and crosscuts were 6.1 m wide, whereas the pillars were square with side dimensions of 12.7 m. Fig. 2 shows the plan view of the room-and-pillar mining layout used in the numerical model and the locations of the four vertical cross-sections, which will be referred to as the cross-sections A1-A1, A2-A2, B1-B1 and B2-B2 to illustrate the numerical modeling results. The dimensions and lithology of the reference model are shown in Fig. 3. The model is based on the case study mine described in Section 2. Fig. 4 shows the locations of three horizontal cross-sections at the immediate roof area, which will be referred to as the cross-sections C-C (roof line), D-D (0.65 m above the roof line) and E-E (1.3 m above the roof line) to illustrate the numerical modeling results.

The laminated nature of the coal mine roof strata makes it crucial to consider the bending and buckling behavior of the thinly bedded layers properly in the numerical modeling. To accurately capture the bending and buckling behavior of the thinly laminated materials at the roof strata, each individual layer is meshed such that at least five overlaying elements are created across the section of each thin layer. The required number of elements across the section width of thinly laminated layers is calculated from performed sensitivity analysis in 3DEC. To increase the accuracy of the calculations, the mesh was refined close to the excavations and gradually was coarsen outwards. The Nodal Mixed Discretization (NMD) scheme was utilized to improve the possible plastic response of the rock mass in the immediate roof area (Itasca, 2013).

The horizontal displacements at the four lateral far field boundaries of the model, as well as the vertical displacement at the bottom of the model were set to zero by prescribing the zero velocity boundary condition.

Since no horizontal stress measurement was done at the mine site, the magnitudes and directions of the principal stresses are not known. Therefore, in this research several parametric studies were performed to examine the response of the model for different possible magnitudes and directions of the horizontal stresses. In the eastern U.S. coalfields, the maximum horizontal stress is generally two to three times the vertical stress, and 76% of the measurements fall within N25°E and N75°E (Agapito and Gilbride, 2002). In the reference model, this ratio was assigned as 2 for the maximum horizontal-to-vertical stress. A stress ratio of 1 was used for the minimum horizontal-to-vertical stress. The direction of the maximum horizontal principal stress was aligned in the direction of the crosscuts (perpendicular to the direction of the entries). A vertical stress of 2.75 MPa was applied to the top of the model to simulate the overburden thickness of 110 m up to the ground level.

3.2. Material and discontinuity models and properties

The failure around underground excavations is a result of failure in both the rock mass part and major discontinuities. In order to realistically predict the failure of the rock mass part, the implemented material constitutive law in the numerical model should

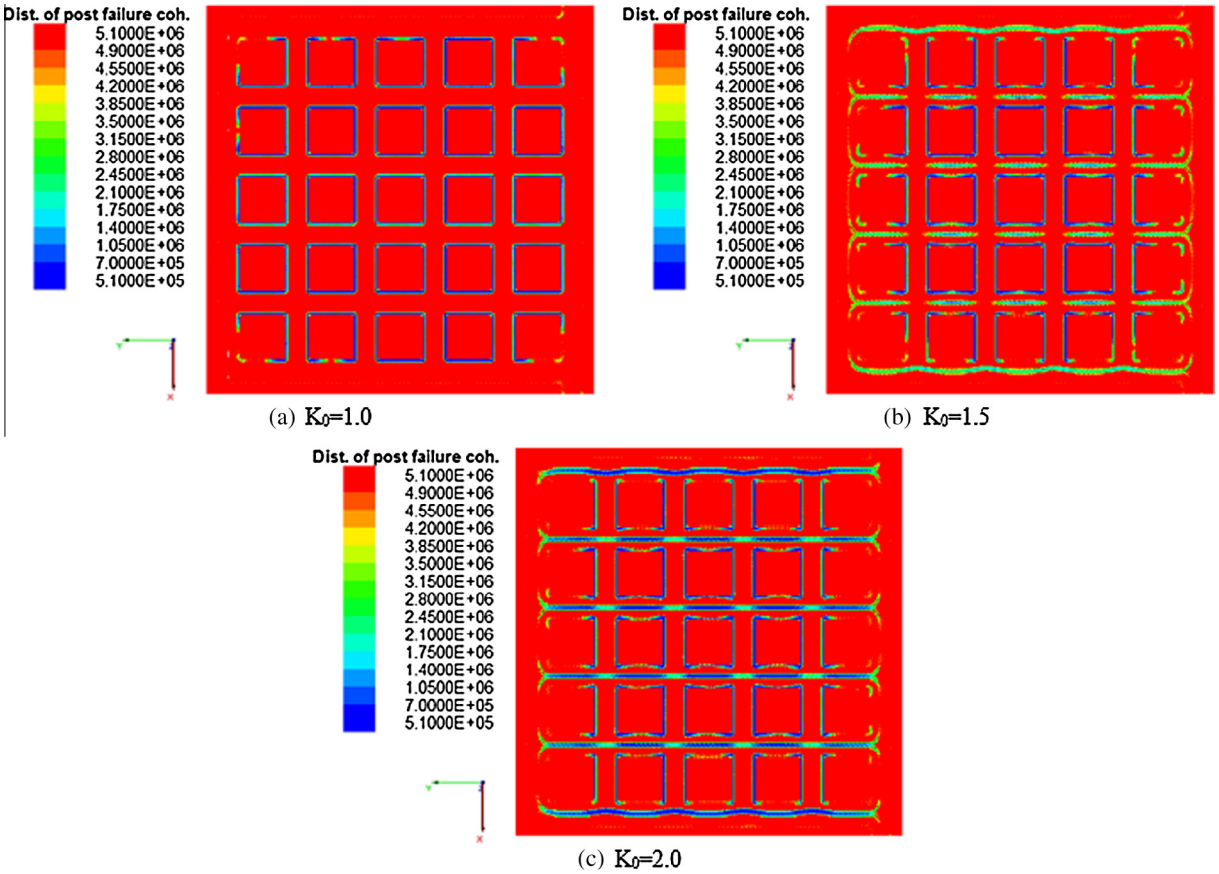

Fig. 7. Distribution of the post failure cohesion at the immediate roof on cross section D-D for different values of K0.

be able to simulate the failure mechanism as closely as possible. Out of the different available material constitutive models, the Mohr-Coulomb elastic perfectly-plastic model is the most commonly used constitutive law in rock engineering designs. In the Mohr-Coulomb model the strength properties of the materials are assumed to remain constant after the onset of plastic failure. This assumption means that the material is able to support a stress equal to the failure strength after failure. In reality, this stress should get transferred to the surrounding zones. Therefore, the Mohr-Coulomb model is only recommended to be applied for the problems where the post failure response of the material is less important. For modeling of the problems such as roof failure where the estimation of plastic strain is required, the strain-softening constitutive behavior is well-suited. The Mohr-Coulomb strain softening model is based on the Mohr-Coulomb model with possible degradation of cohesion, friction angle, tensile strength and dilation after the onset of plastic yield, while in the standard Mohr-Coulomb model those parameters are assumed to remain constant. In this case study, the strain-softening constitutive model was used for the laminated silty shale layer, and for the rest of the materials the standard Mohr-Coulomb constitutive model was assigned. Ideally, the strain softening parameter values should be estimated from laboratory tests. However, in this study, these parameter values were not available and were estimated from a review of parameter values used for modeling of similar problems by Khaled Morsy (2001), Hajiabdolmajid et al. (2002), Salah Badr et al. (2003), Zipf (2006) and Ray (2009). In this research, the friction angle was kept constant, and the cohesion degradation was applied as per Fig. 5 for weak laminated rock.

To account for the scale effect and influence of the presence of minor (small size) discontinuities in the rock masses, the estimated strength and moduli values of the rock materials from lab tests were adjusted to rock mass scale by reducing the mean values of the test results. The Poisson's ratios of the rock masses were increased. In this case study, the results obtained from previous case studies by Kulatilake et al. (2004), Kulatilake and Wu (2013) and Wu and Kulatilake (2012) were used to estimate the rock mass properties from lab test results. The summary of the estimated

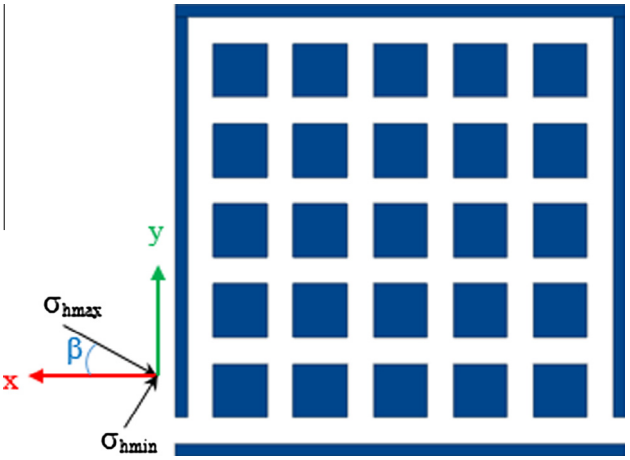

Fig. 9. The maximum horizontal stress direction angle (β) with respect to x-axis.

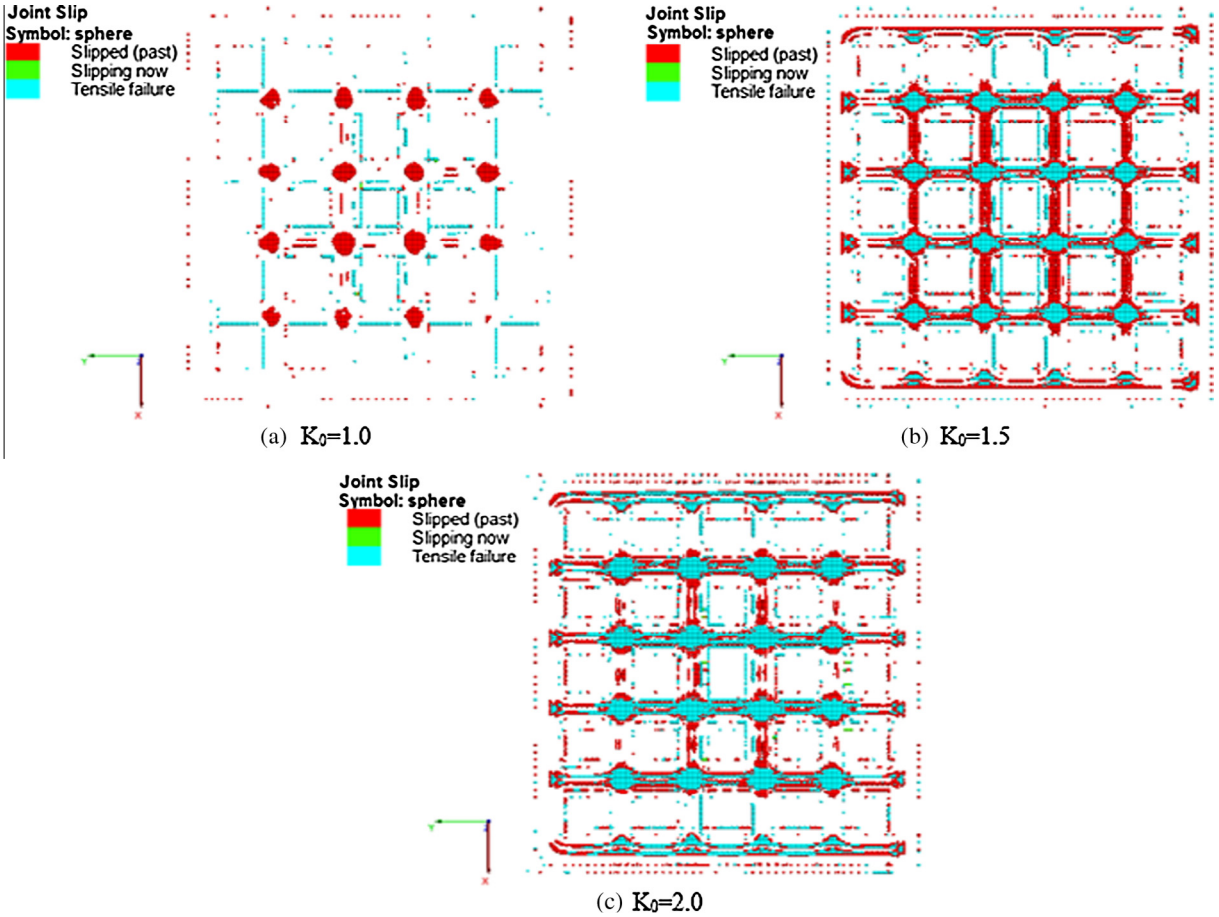

Fig. 8. Failure state of the closest bedding planes to the roofline for different values of K0.

rock mass properties that are used as inputs of the numerical models is given in Table 1. The coal samples were not available for performing laboratory tests, therefore the assigned properties for coal are from a literature review and available test results from the case study mine.

The immediate roof at the case study area is weak laminated silty shale with thin laminations of 2.5–52 mm which fails easily along the weak laminations. For the modeling purposes, the thickness of laminated silty shale and the thickness of laminations are considered as about 4.5 m and 1.0 cm, respectively. With the assumed value for the thickness of laminations, the number of discontinuities needed in the immediate roof would be 450. Meshing the model with this many discontinuities that have very low spacing is an almost impossible task in a large scale model. Therefore, the equivalent continuum concept was used to decrease the number of discontinuities from 450 to 3, by increasing the

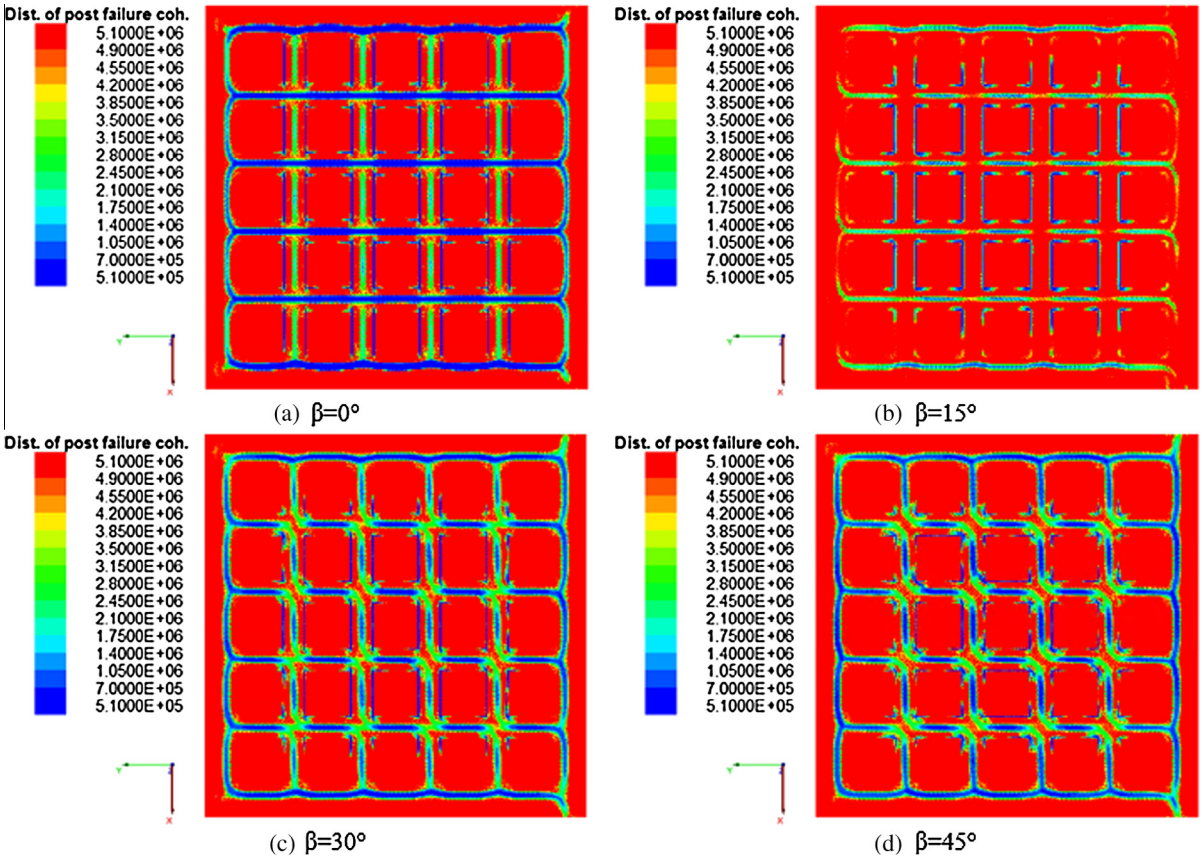

Fig. 10. Distribution of post failure cohesion at the immediate roof on cross section E-E, for different values of β angle.

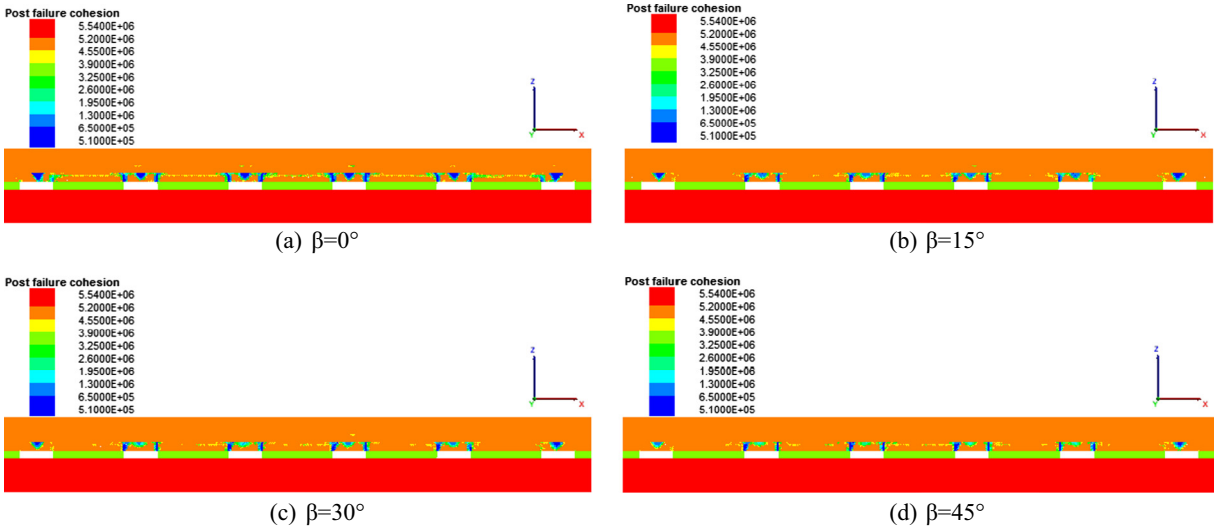

Fig. 11. Distribution of post failure cohesion at the immediate roof on cross section A2-A2 (entries), for different values of β angle.

spacing of the joints from 1 cm to 1.5 m. Based on the equivalent continuum concept, it was necessary to reduce the joint normal stiffness and joint shear stiffness from 61e9 Pa/m and 2.48e9 Pa/m to 4.07e8 Pa/m and 1.65e7 Pa/m, respectively, to obtain the same normal and shear deformations for the laminated silty shale layer with the 3 discontinuities along with the selected new spacing. To be on the conservative side, the shear strength of discontinuities was modeled by a Mohr-Coulomb criterion with a residual friction angle and zero cohesion and tensile strength. Table 2 provides the properties of the discontinuities that were used as input in the numerical modeling.

3.3. Roof failure detection criteria

In 3DEC, the locations of the failures in the rock mass should be judged, for example, by examining plastic indicators (yield flags in 3DEC), grid-point velocities, displacements, localization of shear strain and maximum unbalanced force. In the case of implementing the strain softening behavior, the failure in rock mass damage can be presented as a percentage of cohesion degradation. This allows one to assess the level of the failure that has occurred as a function of accumulated plastic shear strain (Itasca, 2013). In this research, the distribution of post failure cohesion along with other indicators such as the accumulated plastic shear strain and yield state of elements were used to accurately assess the occurrence of failures in the rock mass. In addition, the failure in the discontinuities under both tensile and shear modes were detected through the joint state command.

Table 3
The roof rock strength parameter values used as inputs in the numerical models.

Parameter	Mean value	STD[a]	M[b] + STD	M-STD
Cohesion (MPa)	5.1	0.765	5.865	4.335
Friction angle (°)	21	3.15	24.15	17.85
Tensile strength (MPa)	2.4	0.36	2.76	2.04

[a] STD = Standard deviation.
[b] M = Mean value.

4. Numerical modeling results of parametric studies

4.1. Effect of the maximum horizontal stress magnitude on roof stability

According to the reference case description, a constant vertical normal compressive stress of 2.75 MPa was applied at the top of the model; the minimum horizontal stress-to-vertical stress ratio was kept as one. To assess the influence of the maximum horizontal stress magnitude on stability of the roof, the maximum horizontal-to-vertical stress ratio, K, was increased from K = 1, to 2 in steps of 0.5. The numerical modeling results showed that with increasing K value, the z-displacement increases at the roofline, and for all values of K; the maximum z-displacement occurs above the intersections. For K values greater than 1, the z-displacements above the entries are higher than that above the crosscuts at the roof centers (see Fig. 6). The increase of the maximum horizontal stress magnitude also increases the intensity of shear failure at roof centers above the entries (see Fig. 7).

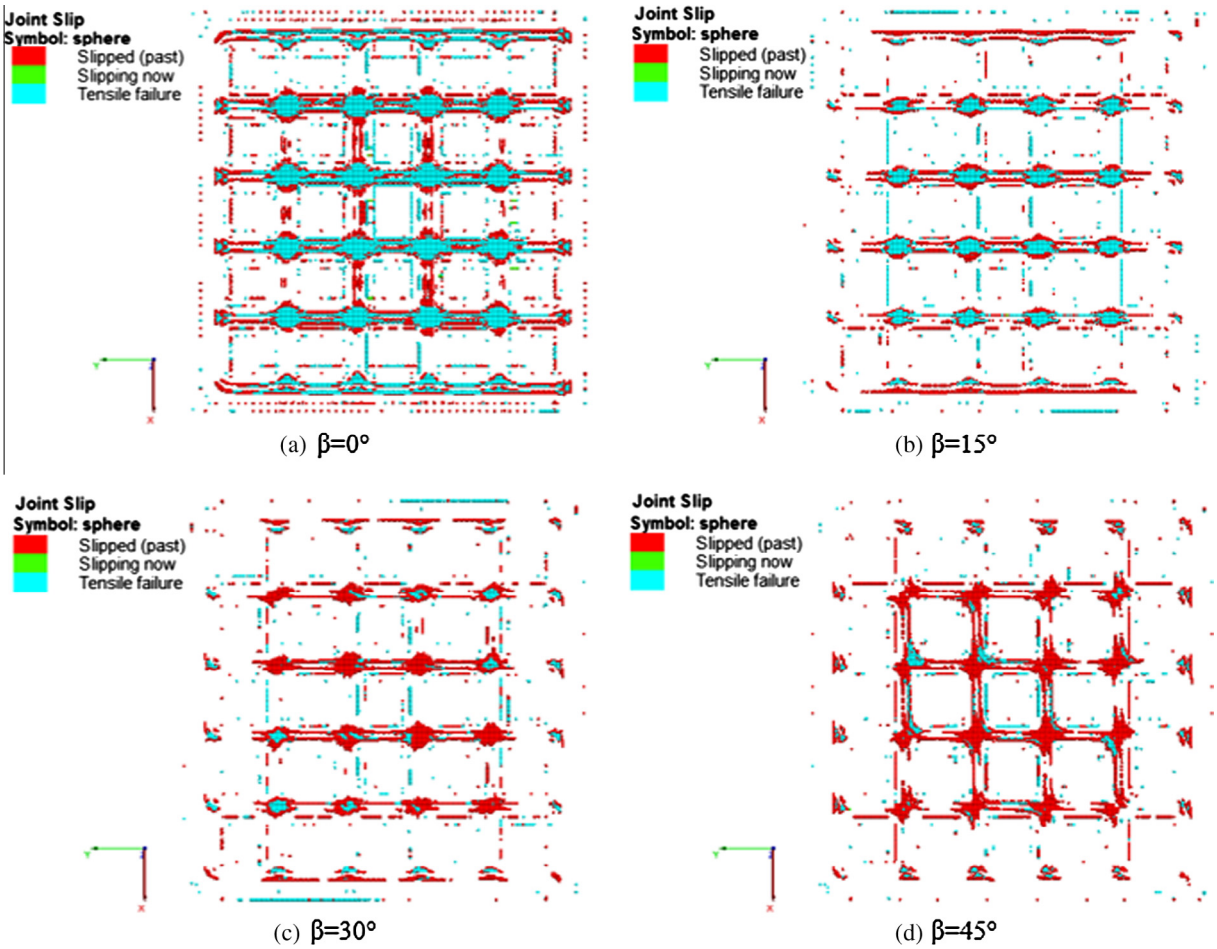

Fig. 12. Failure state of the closest bedding planes to the roofline at different values of β angle.

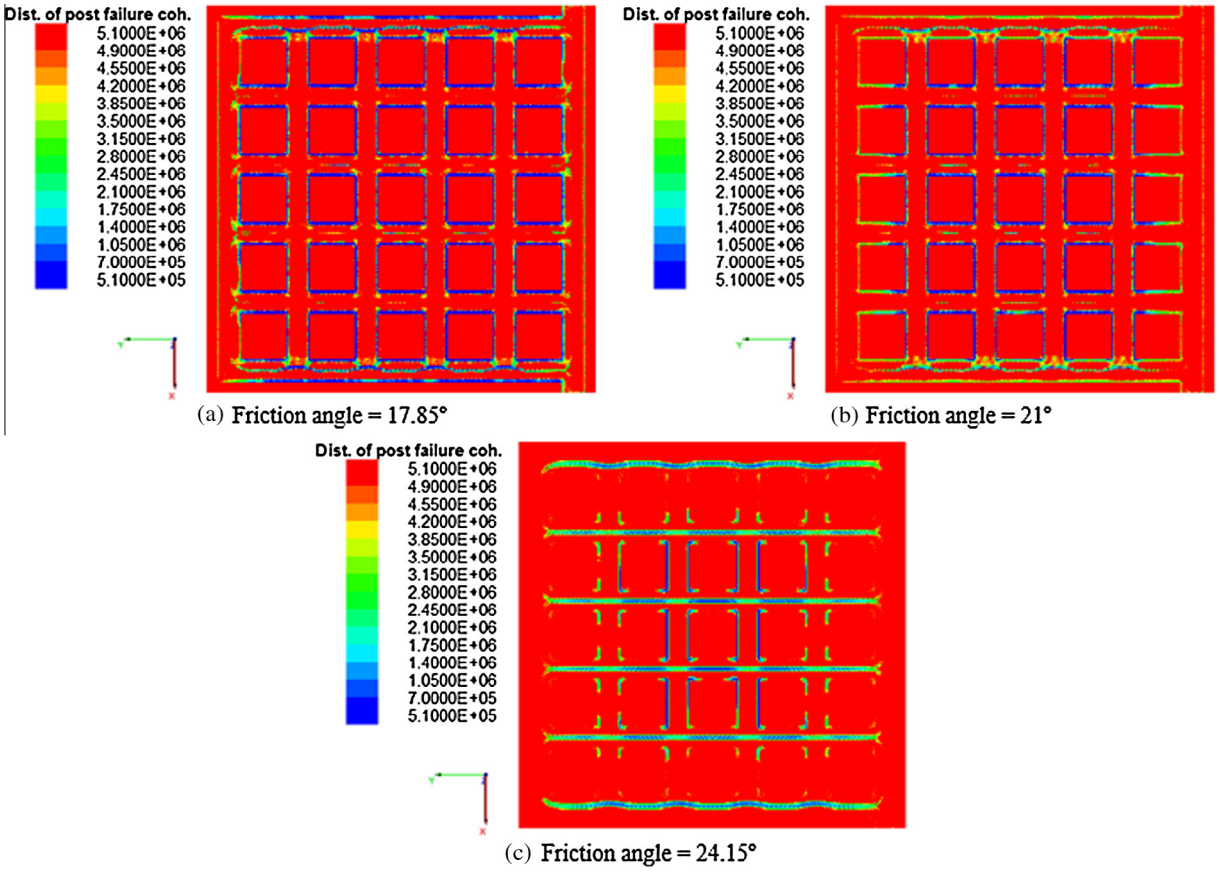

Fig. 13. Distribution of the post failure cohesion at the roofline on cross section C-C for different values of roof rock friction angle.

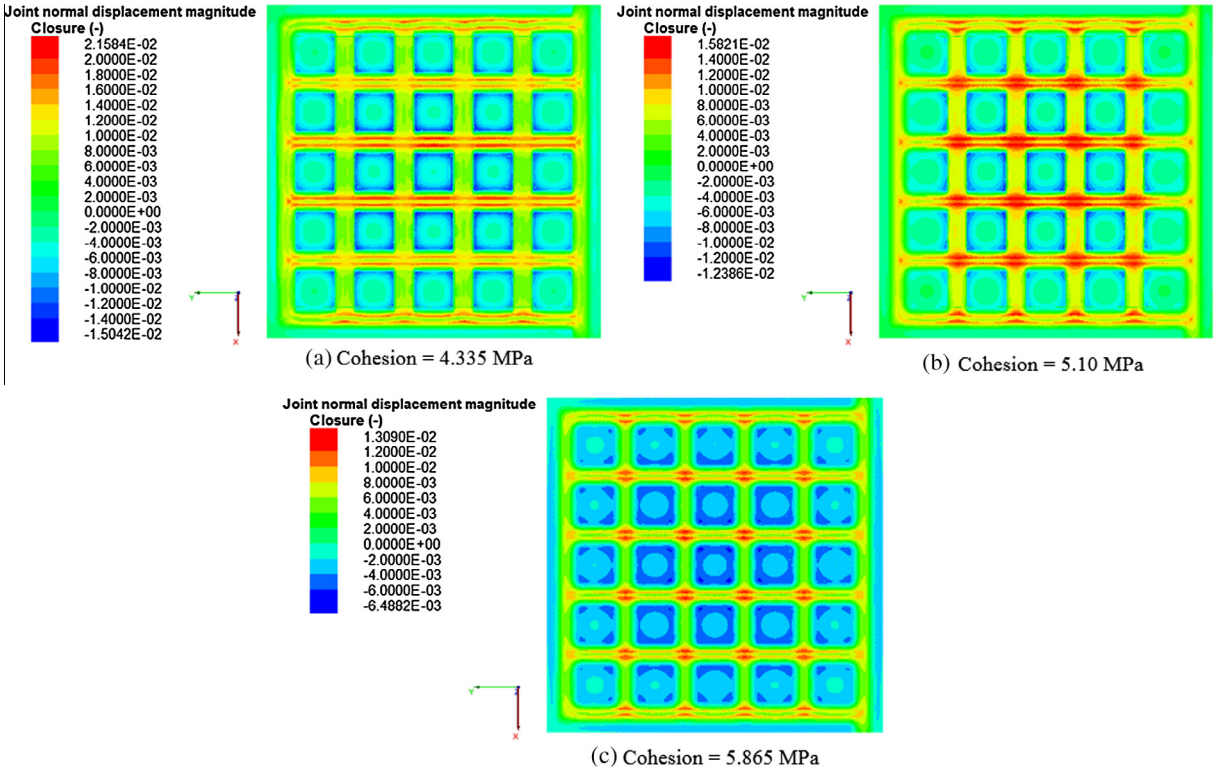

Fig. 14. Joint normal displacement of the closest bedding planes to the roofline for different values of roof rock cohesion.

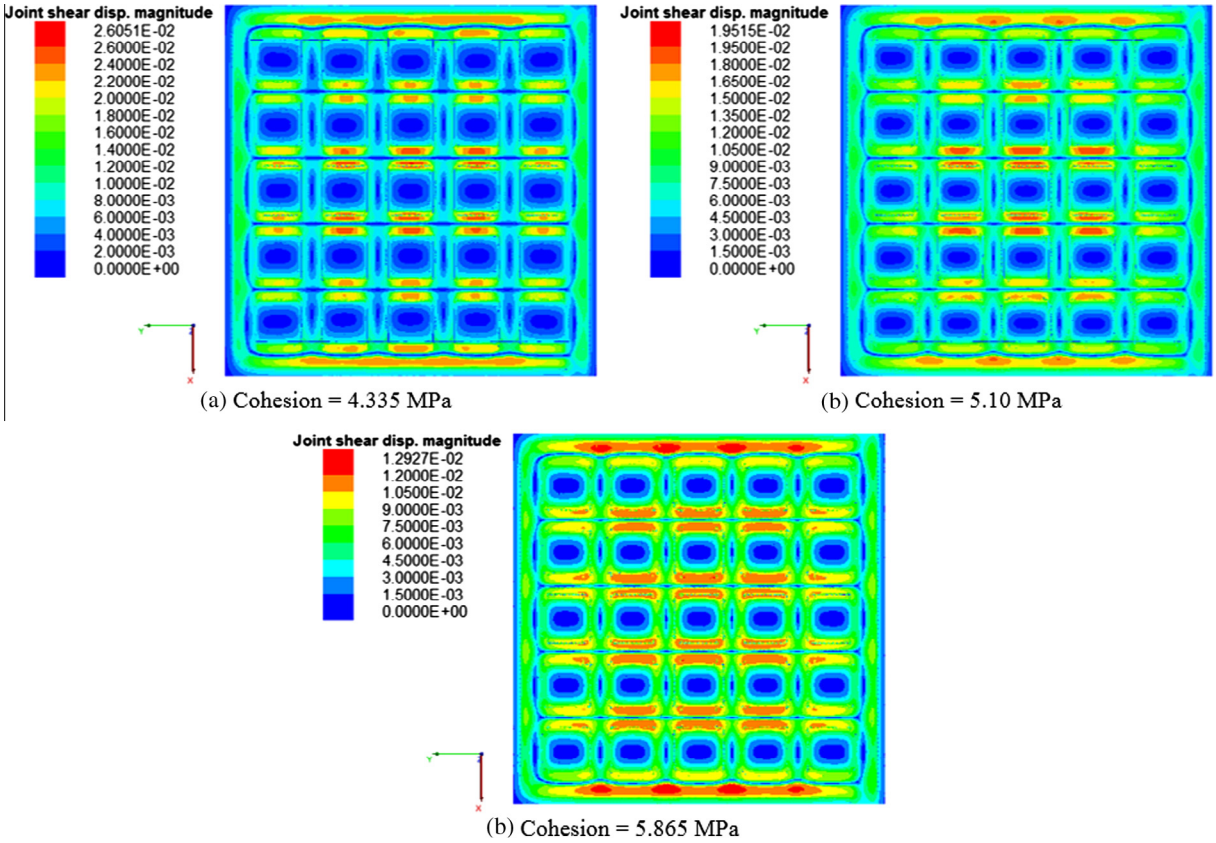

Fig. 15. The joint shear displacement of the closest bedding planes to the roofline for different values of roof rock cohesion.

For all values of K, the maximum separation along the discontinuities takes place above the intersection. The increase of the K value from 1 to 2 increased the magnitudes of the maximum normal and shear displacements along the bedding planes by 7 mm and 9.5 mm, respectively. Fig. 8 shows that with the increase of the maximum horizontal stress magnitude, the intensity of the failures along the bedding planes increases and the type of failure above the intersections changes from shear to tensile. The modeling results described for this parametric study show that for the weak stratified roof, excessive maximum horizontal stress is not the only cause of the cutter roof failure. This type of failure can happen even under the stress regimes with the maximum horizontal stress close to the vertical stress in magnitude, and generally the higher the magnitude of the maximum horizontal stress higher the adverse effect on roof condition.

Fig. 16. Observed roof separation in the field with borehole scope.

4.2. Effect of the horizontal stress orientation on roof stability

The orientation of the maximum horizontal stress has a significant influence on roof stability. The objective of this parametric study was to investigate the influence of the maximum horizontal stress direction on the stability of weak roofs in underground excavations. In this study, the angle between the maximum horizontal stress and the crosscut axis is referred to as the maximum horizontal stress direction angle (β) and was measured with respect to the crosscut axis as shown in Fig. 9. Assuming an increment of 15° for the maximum horizontal stress direction angle, seven cases with angles of 0°, 15°, 30°, 45°, 60°, 75°, and 90° were examined as different possible orientations of the maximum horizontal stress.

The numerical modeling results showed that the variation of the maximum horizontal stress orientation influences the location and severity of the roof failure. With increasing the maximum horizontal stress direction angle, β, the z-displacement decreases at the roofline but still the maximum z-displacement occurs above the intersections. When the maximum horizontal stress is perpendicular to the direction of entries, β = 0°, the z-displacements at the roof centers above the entries are higher than those above the crosscuts. The increase in β angle increases the z-displacement at

Table 4
The discontinuity parameter values used as inputs in the numerical models.

Parameter	Mean value	STD[a]	M[b] + STD	M-STD
Joint friction angle (°)	17.5	2.625	20.125	14.875
Joint normal stiffness (Pa/m)	4.07E+08	6.11E+07	4.68E+08	3.46E+08
Joint shear stiffness (Pa/m)	1.65E+07	2.48E+06	1.90E+07	1.40E+07

[a] STD = Standard deviation.
[b] M = Mean value.

the roof centers above the crosscuts and decreases the z-displacement at the roof centers above the entries. Also, the orientation of the maximum horizontal stress changes the pattern and intensity of failures in the immediate roof area. The intensity of shear failure at roof centers above the entries and above the crosscuts decreases and increases, respectively, with increasing β angle.

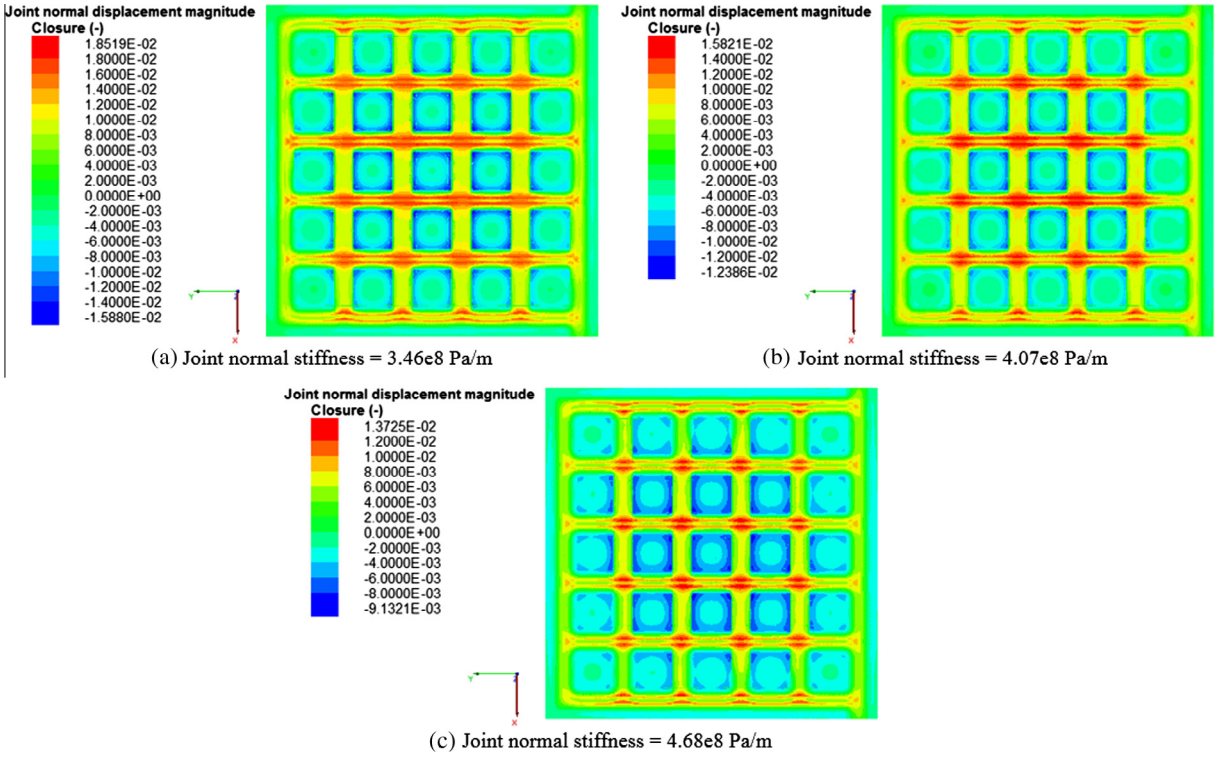

Fig. 17. Joint normal displacement of the closest bedding planes to the roofline for different values of joint normal stiffness.

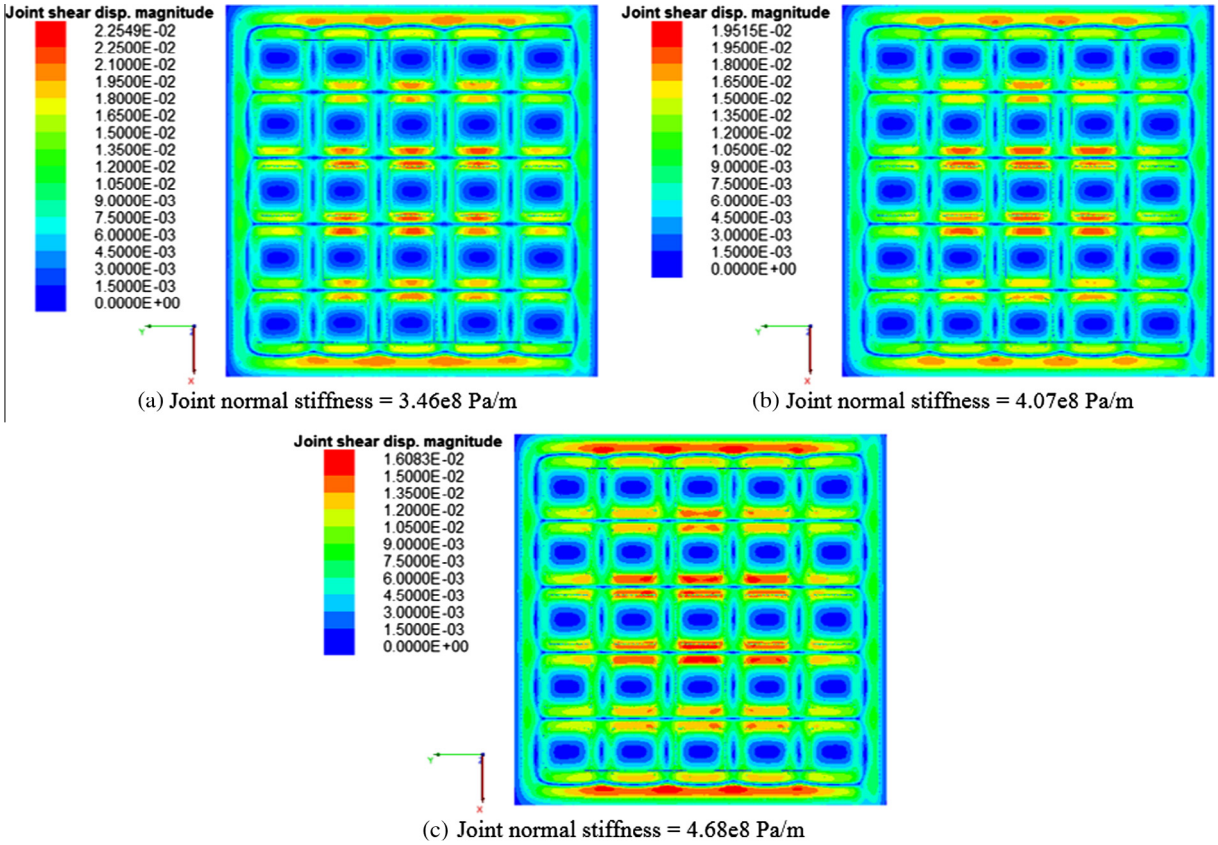

Fig. 18. The joint shear displacement of the closest bedding planes to the roofline for different values of joint normal stiffness.

Table 5
Used room and pillar sizes and the resultant extraction ratios.

Case (#)	Room width (m)	Pillar width (m)	Extraction ratio (%)
Case 1	7.2	11.4	62.4
Case 2	6.1	12.7	54.3
Case 3	5.0	14.0	45.7

The results for β = 30° and 45° show that the shear failures are likely to snake in-between the pillars, and the orientation of shear failures at top of the four-way intersections change with the orientation of the maximum horizontal stress and are nearly in the direction of minimum horizontal stress (see Fig. 10). Offsetting the pillars might help to avoid this type of failure. As was expected, the direction of slippage along the bedding planes has changed with the maximum horizontal stress direction. For β = 45° the roof cutters are more concentrated at a single upper corner of the intersections as opposed to two sides for other values of β angle (see Fig. 11). The magnitude of normal and shear displacements along the bedding planes decreases with increasing the β angle, and for the β = 45° they reach to their minimum values. The intensity of failure along the bedding planes at the immediate roof decreases with increase of the β, and above the intersections the type of failure in bedding planes changes from tensile to shear (see Fig. 12). The numerical modeling results of this parametric study suggests that reorienting the entries to a direction 45° from either the minimum or the maximum horizontal stress can improve the roof condition.

4.3. Effect of the roof rock strength parameters on roof stability

When there is no sufficient data to estimate the standard deviation of geotechnical parameters for variability and uncertainty analysis, as suggested by Duncan (2000), the published values for standard deviation and coefficient of variation can be used. Rethati (1988) suggested a COV ranging between 15% and 20% for geotechnical materials. A small uncertainty would typically be indicated by a COV of 5% while considerable uncertainty would be represented by a COV of 25% (Hoek, 2007). To account for the uncertainty of the rock mass strength parameters, based on a survey of the literature, it is assumed that the coefficient of variation (COV) of the immediate roof rock mass strength parameters of laminated silty shale is about 15%. Using the assumed coefficient of variation, the standard deviations of the cohesion, angle of internal friction and tensile strength of the roof rock mass were calculated. For the numerical modeling, each strength parameter was set to the mean value plus and minus one standard deviation while the other two strength parameters were held at their mean values. Because for the reference case the modeling was performed based on the mean values of the strength parameters, only 6 additional calculations (two for each strength parameter) were needed. Table 3 provides the summary of the roof rock strength parameter values that were used as inputs in the numerical models.

The numerical modeling results showed that the intensity of shear failure at roof lines decreased with the increase of roof rock friction angle and for the highest value of the friction angle, 24.15°, the shear failures are mainly concentrated at central part of the panel and mid span of the entries (see Fig. 13). With the increase of roof rock friction angle from 17.85° to 24.15° in steps of 3.15°, the magnitude of the maximum z-displacement at the roofline decreases from 6.5 cm to 5.1 cm and the magnitude of the maximum normal and shear displacements along the bedding planes reduces by 0.5 cm and 0.7 cm, respectively. The intensity of shear and tensile failures along the bedding planes considerably decreases with the increase roof rock friction angle. The numerical

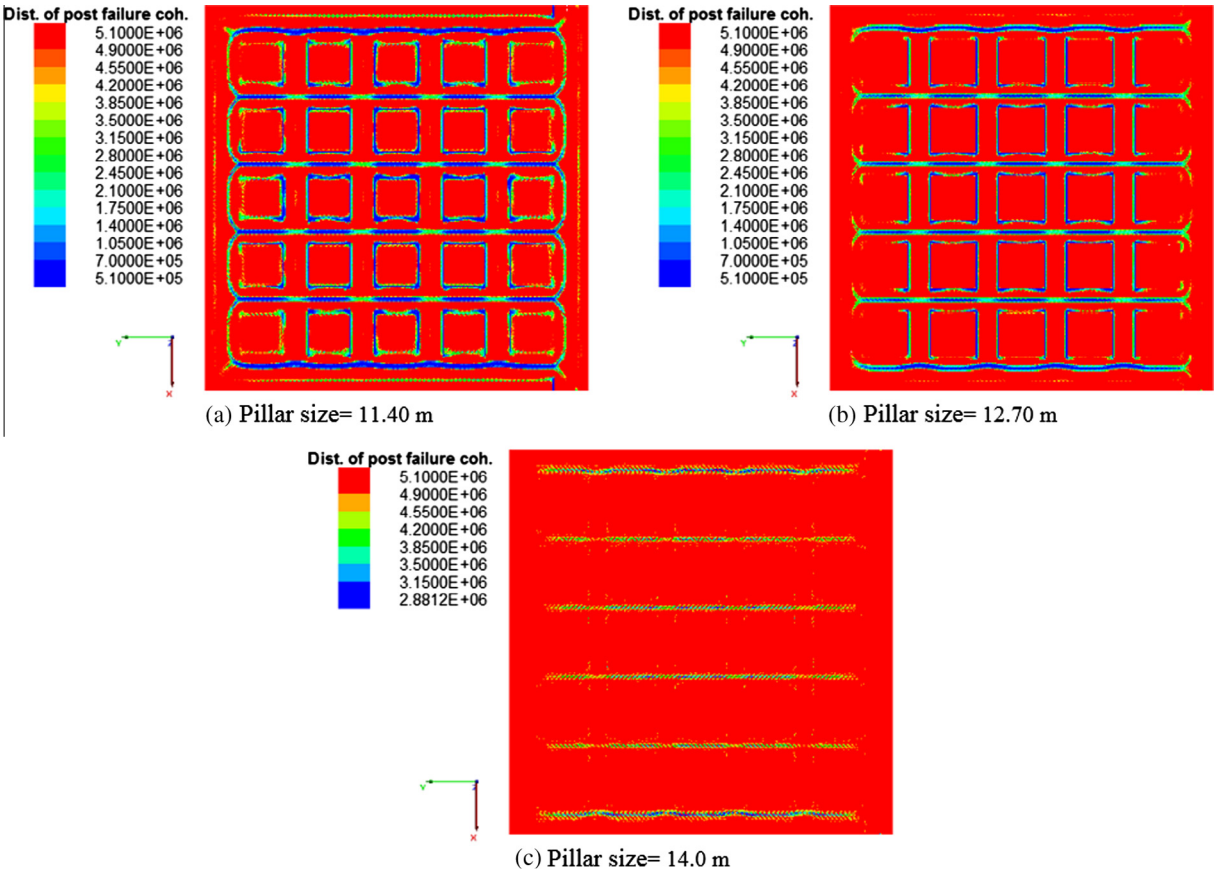

Fig. 19. Distribution of the post failure cohesion at the immediate roof on cross section D-D for different pillar sizes.

modeling results of this parametric study confirmed that the friction angle of the roof rock has a significant impact on the stability of the roof.

The numerical modeling results showed that the increase of roof rock tensile strength from 2.04 MPa to 2.76 MPa in steps of 0.36 MPa, has only minor or negligible effect on all performance measures selected to evaluate the roof stability in this case study.

The magnitude of z-displacement at the roof line, the intensity of shear and tensile failures along the bedding planes, and the intensity of the cutter roof, and shear failure at roof centers above the entries have reduced with the increase of roof rock cohesion value from 4.34 MPa to 5.87 MPa. For the lowest value of the cohesion, 4.34 MPa, the shear failures take place at the upper edges of the entries and crosscuts (cutter roof) as well as at the roof centers above the entries. For the stronger roof compared with the weak roof type, the cutter roof failure at the roof line are more severe in the direction of the minimum horizontal stress above the entries. The magnitudes of the normal and shear displacements along the bedding planes decreases with the increase of roof rock cohesion (see Figs. 14 and 15). From the modeling results it can be concluded that the cohesion of the roof strata has significant influence on the behavior of the roof.

4.4. Effect of the mechanical properties of the discontinuities on roof stability

Field measurements at the case study mine confirmed the occurrence of slip and separation along the interfaces and bedding planes in the laminated roof strata. Fig. 16 shows the roof separation observed with borehole scope which is comparable to numerical model predictions (see Fig. 14b). The bedding planes and interfaces have very low or close to zero tensile strength perpendicular to the discontinuities, and their shear strength is much lower than that of the rock layers. Therefore, due to the stress concentrations caused by excavations, slippage and separation can easily happen along the interfaces and bedding planes before initiation of failure within the rock layers. The intensity of slippage and bed separation in underground openings depends on the rock types as well as the bonding strength of the beds and magnitudes of the loads. The slippage and separation of bedding planes can magnify the adverse effects of stress concentrations around the excavation. Therefore, the bedding planes play an important role on the behavior of roofs in underground excavations, and thinly bedded rock should be considered as a problematic roof in underground excavations.

To account for the uncertainty of the major discontinuity properties, the coefficient of variation (COV) of 15% was adopted. Using the assumed coefficient of variation, the standard deviations for the joint normal stiffness, joint shear stiffness, and joint friction angle were calculated. For the numerical modeling, each parameter was set to the mean value plus and minus one standard deviation, while the other two parameters were held at their mean values. Table 4 provides the summary of the discontinuity parameters that were used as inputs in the numerical models.

The numerical modeling results show that for all three assigned friction angles (14.8°, 17.5°, and 20.1°) the shear failures are happening in the bedding planes. As expected, the shear failure along the bedding planes has decreased with the increase of the bedding

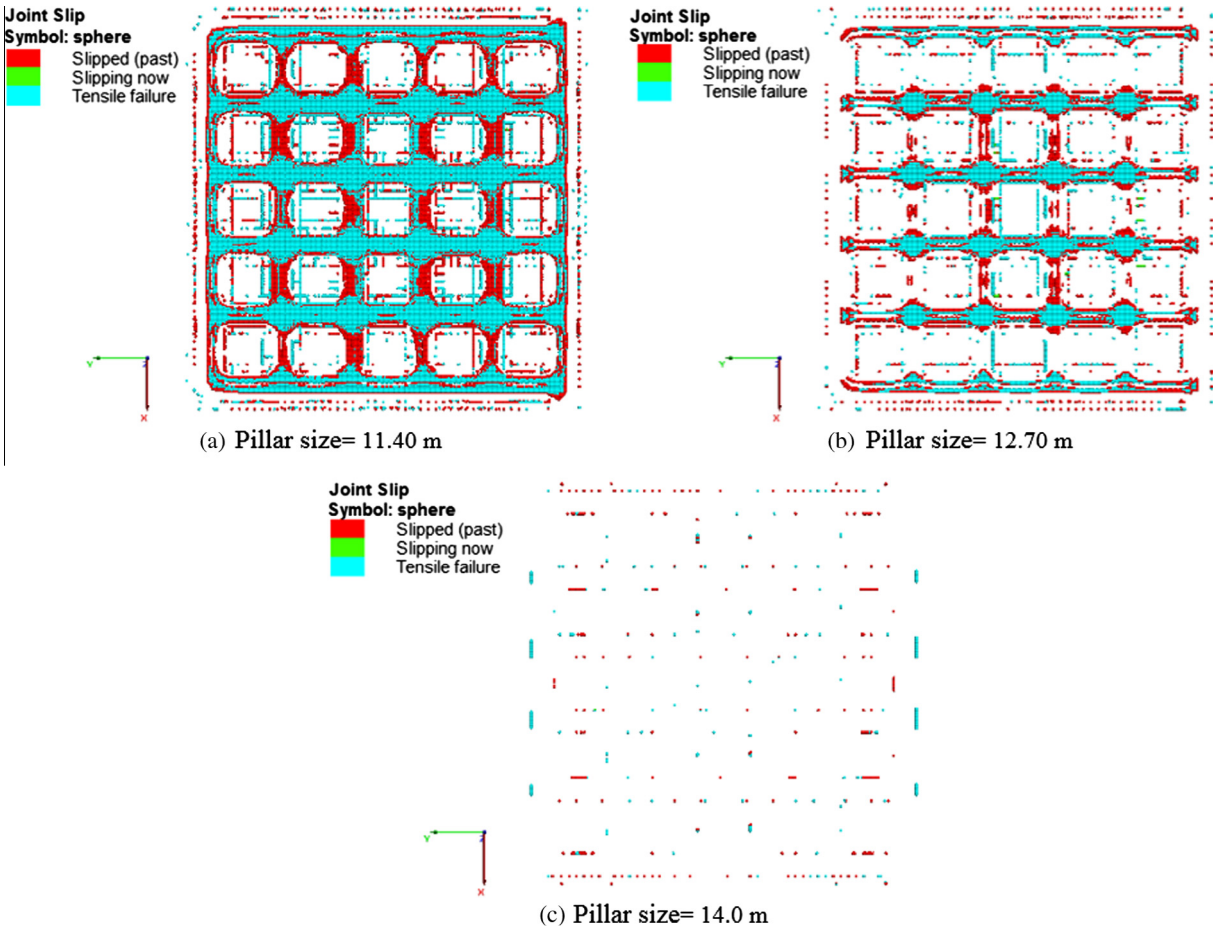

Fig. 20. Failure state of the closest bedding planes to the roofline for different pillar sizes.

plane friction angle. The changes in the elastic and plastic behavior of the immediate roof were negligible for different assigned bedding friction angles.

With the increase of normal stiffness of the bedding planes from 3.46e8 Pa/m to 4.68e8 in steps of 6.11e7 Pa/m, the magnitude of the maximum z-displacement at the roof line decreases from 6.4 cm to 5 cm. The intensity of the cutter roof failures decreases as the joint normal stiffness value increases. Finally, the magnitude of the normal and shear displacements as well as the intensity of shear and tensile failures along the bedding planes decrease with the increase of the joint normal stiffness value (see Figs. 17 and 18). From the numerical modeling results it can be concluded that the joint normal stiffness value has a significant influence on roof stability.

The increase of the shear stiffness of bedding planes from 1.40e7 Pa/m to 1.90e7 Pa/m in steps of 2.5e6 Pa/m had a negligible effect on all performance measures selected to assess roof stability in this case study; it only slightly decreased the shear displacement along the bedding planes.

4.5. Effect of variation of room and pillar size on roof stability

In room-and-pillar mines, the relation between the room and pillar sizes is known as the extraction ratio. The increase (decrease) in the pillar size results in a decrease (increase) in the room size and therefore, the extraction ratio decreases and increases respectively with the increase and decrease of the pillar size. To study the influence of the pillar and room sizes on stability of the roof, three different models were simulated. In the first case, the pillar width of the reference case was increased by 10%, and in the second case, it was decreased by the same amount, see Table 5.

With the increase of pillar size from 11.40 m to 14.0 m in steps of 1.30 m, the magnitude of the maximum z-displacement at the roofline decreased from 7.5 cm to 3 cm, and the magnitude of the maximum normal and shear displacements along the bedding planes reduced by 1.47 cm and 1.69 cm, respectively. The intensity of shear and tensile failures along the bedding planes, and the intensity of the cutter roof, and shear failure at roof centers above the entries have reduced significantly with the increase (decrease) of pillar (room) size (see Figs. 19 and 20).

5. Summary and conclusions

In the presence of discontinuities, the distribution of stresses and deformations induced in a rock mass can differ significantly from those predicted by continuum based techniques. The deformation modulus, strength and stress-strain responses of discontinuous rock masses can all be affected by discontinuities in a nonlinear and anisotropic manner. The homogenization and combined continuum–interface approaches are two commonly employed procedures in continuum based methods to account for the presence of discontinuities in rock masses. However, the methods based on these approaches are limited by the fact that the deformation mechanisms involving movements such as separation, slip and rotation of blocks cannot be modeled properly by these methods. Therefore, realistic modeling of the mechanical behavior of discontinuities is essential for successful numerical modeling of discontinuous rock masses. The employed numerical technique should be able to capture the broad range of rock mass behaviors caused by interactions between the different rock masses (which consists of intact rock and minor discontinuities), major discontinuities and support system. In contrast to the continuous based methods, distinct element methods provide more accurate and realistic description of the physical behavior of discontinuous rock masses. In this paper, the three-dimensional distinct element method was used to investigate the stability of the roof in an underground room-and-pillar coal mine and the implemented technique was able to accurately capture the possible failure of the major discontinuities and the rock mass part consist of intact rock and minor discontinuities.

In summary, the research conducted in this paper showed that the bedding planes play an important role on the geo-mechanical behavior of roof in underground excavations. Therefore, an appropriate numerical modeling technique which incorporates the effect of discontinuities should be employed to simulate the realistic behavior of the discontinuous rock masses such as the layered materials in roof strata of the underground coal mines. The three-dimensional distinct element method used in this research showed the capability of this technique in capturing the important geo-mechanical behavior around underground excavations. The laboratory tests are essential for determination of intact rock and discontinuity properties to make accurate predictions of real world underground stability problems. The roof failure in underground excavations is most likely a progressive failure that starts at the weakest part of the rock mass where the stress concentrations are higher than that of the roof rock strength and then propagates in the least resistance path within the rock mass. The roof failure in underground excavations is a progressive failure which has been successfully modeled numerically using the strain-softening constitutive model because the standard Mohr-Coulomb model is unable to fully capture the post-failure behavior of the rock masses.

Acknowledgements

The support provided by the mining company through providing geological data, rock core and block samples, and allowing access to the mine to perform field investigations is very much appreciated. The work was funded by the NIOSH of the Centers for Disease Control and Prevention (Contract No. 200-2011-39886).

References

Agapito, J., Gilbride, L., 2002. Horizontal stresses as indicators of roof stability. In: SME Annual Meeting, February, Phoenix, Arizona.

Chen, H., 1999. Stress Analysis in Longwall Entry Roof Under High Horizontal Stress. West Virginia University Libraries.

Duncan, J.M., 2000. Factors of safety and reliability in geotechnical engineering. J. Geotech. Geoenviron. Eng. 126 (4), 307–316.

Gadde, M., Peng, S., 2005. Numerical simulation of cutter roof failure under weak roof conditions. In: 2005 SME Annual Meeting: Mining Preprints, pp. 459–469.

Hajiabdolmajid, V., Kaiser, P., Martin, C., 2002. Modelling brittle failure of rock. Int. J. Rock Mech. Min. Sci. 39 (6), 731–741.

Hoek, E., 2007. Practical Rock Engineering. <http://www.rocscience.com/hoek/corner/Practical_Rock_Engineering.pdf> (Apr. 4, 2012).

Itasca, 2013. Three-Dimensional Distinct Element Code, Ver. 4.1. Itasca, Minneapolis.

Khaled Morsy, S.S.P., 2001. Typical complete stress-strain curves of coal. In: 20th International Conference on Ground Control in Mining. Morgantown, West Virginia.

Kulatilake, P.H.S.W., Park, J., Um, J., 2004. Estimation of rock mass strength and deformability in 3-D for a 30 m cube at a depth of 485 m at Aspo Hard Rock Laboratory. Geotech. Geol. Eng. 22, 313–330.

Kulatilake, P.H.S.W., Wu, Q., 2013. REV and equivalent continuum/discontinuum 3-D stability analyses of a tunnel. In: Proceedings of the 3rd International FLAC-DEM Symposium, China. Paper received a Peter Cundall Award.

Ray, A.K., 2009. Influence of cutting sequence on development of cutters and roof falls in underground coal mine. In: 28th International Conference on Ground Control in Mining. Morgantown, WV.

Rethati, L., 1988. Probabilistic solutions in geotechnics. Developments in Geotechnical Engineering, vol. 46. Elsevier, Amsterdam.

Salah Badr, R.M., Kieffer, S., Salamon, M.D.G., Ozbay, U., 2003. Numerical modeling of longwalls in deep coal mines. In: 22nd International Conference on Ground Control in Mining. Morgantown, West Virginia.

Wu, Q., Kulatilake, P.H.S.W., 2012. REV and its properties on fracture system and mechanical properties, and an orthotropic constitutive model for a jointed rock mass in a dam site in China. Comput. Geotech. 43, 124–142.

Zipf, R., 2006. Numerical modeling procedures for practical coal mine design. In: Proc. of the 41st US Rock Mechanics Symposium, Golden, Colorado.